ELSEVIER

Journal of Alloys and Compounds 459 (2008) 261–266

Journal of ALLOYS AND COMPOUNDS

www.elsevier.com/locate/jallcom

A combinatorial study of the corrosion and mechanical properties of Zn–Al material library fabricated by ion beam sputtering

Wei Chen [a], Qingfeng Liu [a], Qian Liu [a,*], Lihui Zhu [b], Li Wang [c]

[a] *State Key Laboratory of High Performance Ceramics and Superfine Microstructure, Shanghai Institute of Ceramics, Chinese Academy of Sciences, Shanghai 200050, China*

[b] *Department of Materials Engineering, Shanghai University, Shanghai 200072, China*

[c] *Technology Center, Baoshan Iron & Steel Co. Ltd., Shanghai 201900, China*

Received 12 April 2007; received in revised form 8 May 2007; accepted 9 May 2007
Available online 16 May 2007

Abstract

A combinatorial method was utilized to fabricate a Zn–Al material library by ion beam sputtering. The material library was produced by manipulating the position of substrate and moving shutters to deposit multilayer metal films. As-deposited films were annealed at low temperatures to form through-thickness homogenous films. Different annealing conditions were studied and high quality alloy films could be obtained by annealing at 370 °C. Electrochemical corrosion properties of the material library were evaluated by a modified tape test. Results of the electrochemical tests show that the Zn–Al film with a composition of 72.6 wt% Al has the best anti-corrosion properties in the material library. Nanoindentation tests were conducted to investigate the mechanical behaviour. Zn–Al films containing a high content of Al possess better mechanical properties with a high hardness and elastic module.

Keywords: Coating materials; Vapour deposition; Corrosion; Mechanical properties

1. Introduction

Zinc coatings have been widely used for decades to provide corrosion protection for metal structures exposed to natural atmosphere. These coatings act as barriers as well as sacrificial anodes to prevent their protected substrates from becoming useless rust. However, it is seldom satisfactory for zinc coatings to meet the more demanding anti-corrosion needs in severer industrial or marine atmosphere. A range of Zn–Al coatings were thus developed as replacements for zinc coatings [1]. Although a complete understanding of the function mechanism of Zn–Al coatings is still in progress [2], the formation of insoluble corrosion products and preferential corrosion phenomena were generally believed to be the reasons for the superior performance of Zn–Al coatings [3–5].

Several techniques have been employed to apply Zn–Al coatings, including electroplating [6], thermal spray [7] and hot-dip [8]. Galvalume (Zn–55 wt% Al) and Galfan (Zn–5 wt% Al) are two of the most commercially successful Zn–Al coatings, both of which are produced by a continuous hot-dip process. The hot-dip process for Zn–Al coatings is well established, but environmental concerns and energy cost cloud the future of this technology. Electrochemical deposition also faces similar issues. On the other hand, PVD methods such as sputtering are prospective in that they can produce high quality films, which attain the same protection effect with a much reduced thickness [9]. Meanwhile, these methods are environmental friendly and energy efficient [10].

The main objective of the study was to get a better understanding of the effect of composition on the mechanical and corrosion properties of PVD Zn–Al films. A combinatorial method was utilized to deposit a Zn–Al material library containing samples of different compositions by an ion beam sputtering. The conventional method of one-by-one deposition requires repeated time-consuming target fabrications, vacuum evacuations and deposition processes, but for the combinatorial approach, a high speed parallel synthesis of film samples can dramatically reduce preparation time and improve research efficiency

* Corresponding author. Tel.: +86 21 5241 2612; fax: +86 21 5241 3122.
E-mail address: qianliu@sunm.shcnc.ac.cn (Q. Liu).

0925-8388/$ – see front matter © 2007 Elsevier B.V. All rights reserved.
doi:10.1016/j.jallcom.2007.05.046

[11–13]. Another objective of the research is thus to develop a combinatorial method to screen and optimize the Zn–Al alloy films for their anti-corrosion application.

2. Experimental method

2.1. Combinatorial fabrication of Zn–Al material library

An ion beam sputtering system with a 3 in. Kaufman ion source was employed to deposit the Zn–Al material library. The system has a deposition chamber with a base pressure less than 10^{-8} Torr and a load-lock chamber to replace substrates without breaking the vacuum in the deposition chamber. Mild carbon steel and Si(0 0 1) wafers of 1 in. × 1 in. were used as substrates. The steel substrates were ground and polished to a surface roughness of 0.5 μm. Finally, they were degreased ultrasonically in methanol and acetone before loading into the deposition chamber. Pure Zn and Al targets (purity 99.99%) were mounted and pre-sputtered for 15 min to remove the contaminated surface layers and stabilize the surface condition.

The material library was deposited as discrete multilayered films on unheated substrates. Ar ions with an acceleration voltage of 1 keV and a current of 25 mA were used as the incident beam. The spatial variation of composition was created by controlling the ratio of element layers at different regions of the substrates (Fig. 1). A mask with a predefined matrix was placed over the substrate to facilitate later sample identification. A sequence of Al depositions was then carried out along the *x*-axis of the substrate by moving a computer-controlled shutter over the mask, exposing different columns to be deposited with films of stepwise thickness. This was followed by a substrate rotation and another sequence of Al depositions along the *y*-axis. After finishing Al layer, Zn deposition was conducted in similar procedures. A double layer of Zn and Al, totally 500 nm, was fabricated in one round. To achieve samples of larger thickness, multiple double layers were deposited. The deposition rates for Zn and Al were 2.3 Å/s and 1.2 Å/s, respectively as was monitored by an in situ quartz crystal balance. Films of 1 μm thickness were used in structure and property characterization. As-grown multi-layered films were annealed in Ar/H_2 (5%) atmosphere to obtain a full compositional mixing normal to the film plane. The content of Zn or Al can be calculated by the film thickness and theoretical density values.

2.2. Structure and composition characterization

Surface and cross-section morphologies of the as-deposited and annealed samples from selected regions together with the chemical composition of the library were studied and determined on a JEOL 6700F SEM with X-ray spectrometry (EDS). Auger depth profile analyses were performed to examine the through thickness chemical uniformity on a VG MICROLAB-310F field emission auger system. X-ray diffraction (XRD) was utilized to identify the phase components of different samples in the material library. XRD patterns were collected with a Rigaku D/max2550V diffractometer using Cu Kα radiation (40 kV and 60 mA) with a scan step of 0.02° and a scan rate of 0.12°/s.

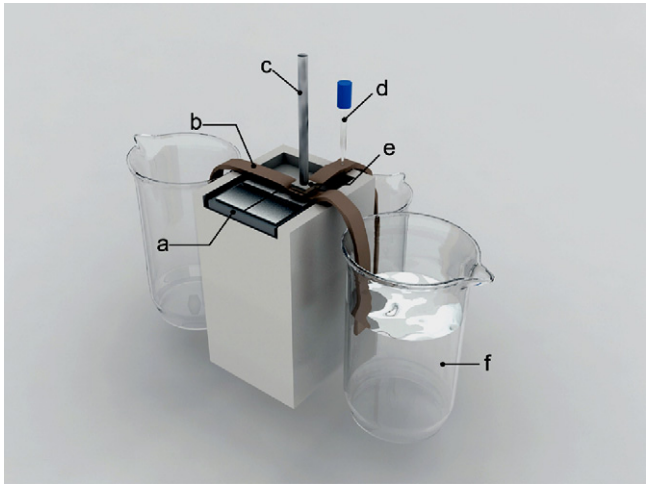

Fig. 2. Scheme of the tape test arrangement (a) material library, (b) textile tape, (c) glass rod, (d) reference electrode, (e) counter electrode, and (f) electrolyte.

2.3. Evaluation of electrochemical corrosion behaviour

The corrosion resistance was measured by a modified tape test (Fig. 2) [14]. In the test arrangement, the electrolyte (3.5% NaCl, near neutral) was made to flow slowly from one beaker to another using a multilayered textile tape. A portion of the wet tape was pressed against the specimen surface by a glass pod. Only the area covered by the tape is exposed to the electrolyte. A Pt counter electrode of the same size as the testing area was pushed on the opposite side of the tape. The size of the working electrode was 16 mm^2. The reference electrode was a saturated calomel electrode (SCE) in a Luggin capillary. The electrochemical measurements were performed on a CHI760C electrochemical workstation. Samples in the material library were screened by their polarization resistance and corrosion potential. Potentiodynamic polarization tests were also conducted on selected samples at a scanning rate of 20 mV/min. All tests started after the electrolyte flow over the sample was steady.

2.4. Evaluation of mechanical performance

Mechanical properties as a function of composition were measured by nanoindentation. A CSM nano hardness tester with a Berkovich diamond indenter tip was operated in a linear loading mode at a loading rate of 10 mN/min and

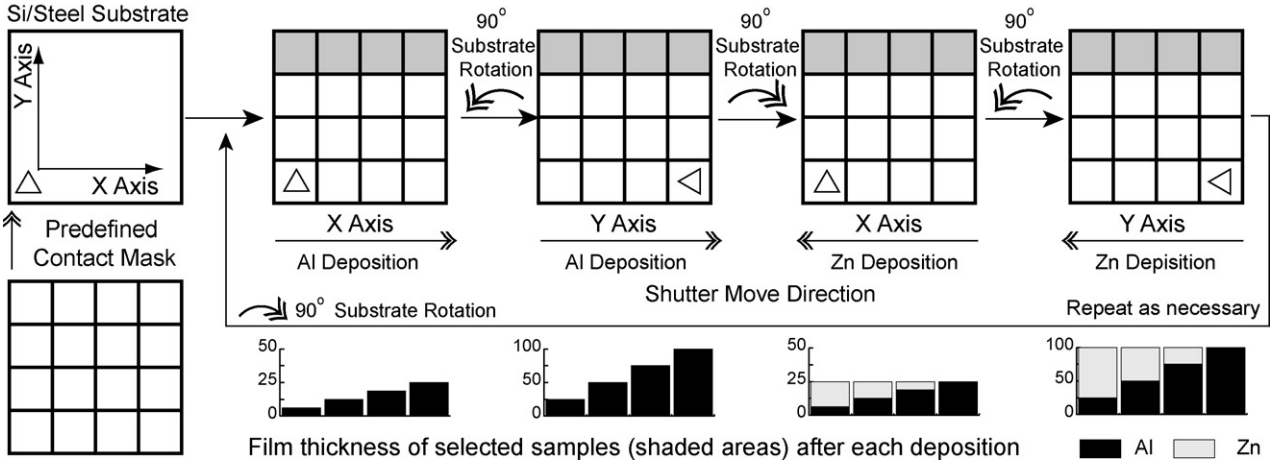

Fig. 1. Steps of combinatorial deposition of Zn–Al material library by ion beam sputtering.

a maximum load of 5 mN. The reported results were the average of 20 indents. The hardness and reduced modulus were derived from the unloading portion of the load–displacement curve following the procedures by Oliver and Pharr [15].

3. Results and discussion

3.1. Synthesis and characterization of Zn–Al material library

A suitable annealing process is necessary to attain a complete through-thickness mixing of the metal layers for an effective material library [16]. At higher temperatures, the evaporation of Zn will cause the composition change in specimen. But at lower temperatures, the annealing time had to be extended, which would introduce more defects and large amount of substrate element (especially for Si) in the alloy films. The time required for the layers to fully interdiffuse was estimated by published diffusion data [17]. The annealing temperature for the Zn–Al library was selected at 370 °C by our preliminary research. Typical diffusion coefficient for Zn–Al system is of the order of 10^{-15} m^2 s^{-1} at the annealing temperature of 370 °C, which suggested that at least 2 h are required for a multilayer film of 2 μm in thickness.

A Zn–Al sample, with a uniform layer thickness of about 250 nm each and a total thickness of 2 μm on a silicon substrate, was prepared to examine the extent of the interdiffusion after heat treatment. Fig. 3 shows cross section SEM backscatter electron images of an "as-deposited" sample and samples after 2-h annealing in Ar/H_2 atmosphere at 370 °C and 470 °C. In Fig. 3(a), as-deposited metal layers are distinguishable in the SEM image. The interfaces between the dark Al layer and the bright Zn layer are relatively flat. The appearance of the layers changes dramatically in Fig. 3(b). Based on AES depth profile of this sample, the film is a uniform mixture of Al and Zn except for an oxide surface layer with thickness of no more than a few nanometers. Fig. 3(c) shows the roughness and porosity of the outer Zn–Al film increases with higher annealing temperature. There is a Zn-rich layer appearing on the interface between the silicon substrate and the Zn–Al film.

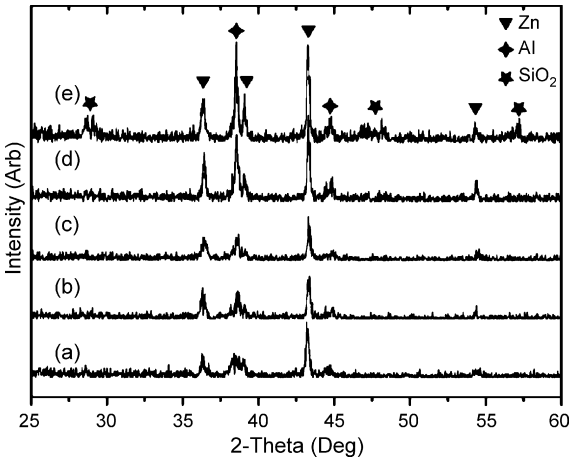

Fig. 4. X-ray diffraction pattern for: as-deposited multilayer Zn–Al films on silicon substrate (a), and after annealing 2 h at 320 °C (b), 370 °C (c), 420 °C (d) and 470 °C (e).

Fig. 4 is the X-ray diffraction patterns for the as-deposited film and films annealed at different temperatures. Compared with the results of the as-deposited sample [Fig. 4(a)], XRD patterns of the annealed samples do not change very much when heat-treated at 320 °C and 370 °C [Fig. 4(b) and (c)]. The results show annealing at these temperatures mainly facilitates the interdiffusion of the different compositions. A significant increase in the XRD peak intensities is observed for the 420 °C and 470 °C annealed sample [Fig. 4(d) and (e)]. This reveals that annealing at relative high temperatures can lead to an improved crystallinity. Some trace of XRD peaks for silicon dioxide can be identified from the sample annealed at 470 °C. The detailed research has not been conducted on this issue, but it can be concluded that high temperature annealing will complex the film–substrate interaction and bring unexpected results.

The XRD patterns for the samples annealed at 370 °C and 470 °C on steel substrates are shown in Fig. 5. When annealed at 370 °C, the samples were still Zn–Al binary system with no peaks for intermetallic phase detected [Fig. 5 (a)]. As for the 470 °C annealed samples, the peaks corresponding to Fe_4Zn_9 were identified in the pattern [Fig. 5(b)]. The formation of Fe–Zn intermetallics can improve the film–substrate adhesion

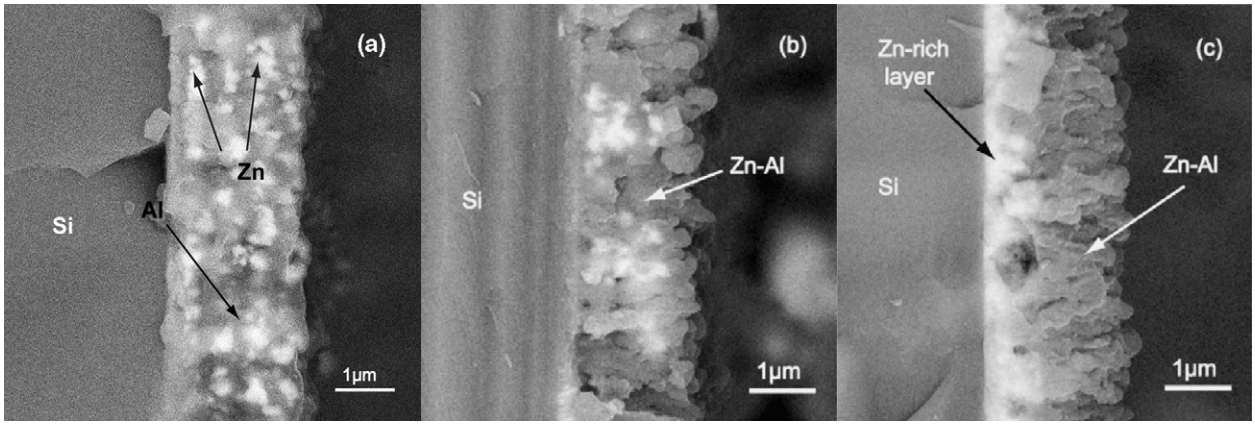

Fig. 3. Cross-sectional SEM backscatter electron image of Zn–Al film on Si substrate: as-deposited multilayered film (a) and after annealing in Ar/H_2 atmosphere for 2 h at 370 °C (b) and 470 °C (c).

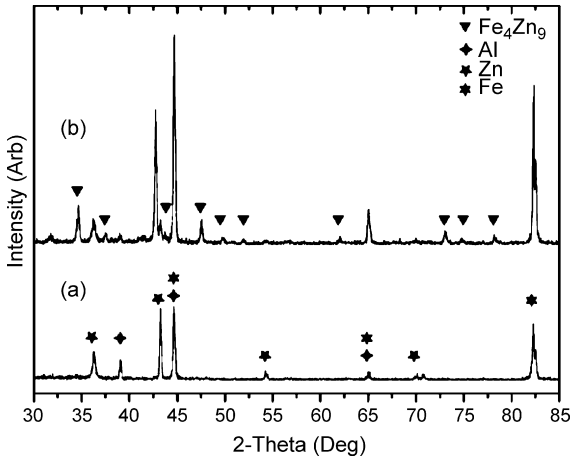

Fig. 5. X-ray diffraction pattern for Zn–Al films on low carbon steel substrate annealed 2 h at 370 °C (a) and 470 °C (b).

and weldability, but it reduces the corrosion performance of the film [8,18].

3.2. Electrochemical corrosion properties

Fig. 6 shows the polarization resistance and corrosion potential for samples in the Zn–Al material library as a function of Al content. The polarization resistance was determined by the slope of linear potential–current density curve where current density is zero. The corrosion current density, i_{corr}, can be related to the polarization resistance R_p by the Stern–Geary coefficient, B [19]:

$$R_p = \left(\frac{\partial \Delta E}{\partial i}\right)_{i=0,\, dE/dt \to 0} = \frac{B}{i_{corr}} \quad (1)$$

Polarization resistance measurement enables a fast evaluation of corrosion properties for material library within a potential range that is similar to the actual corrosion process. The smallest value of polarization resistance R_p(about 200 Ω/cm^2) for the entire Zn–Al composition appears when the volume percent of Al is over 20 vol.% (note: volumetric percentage in the as-deposited multilayer film was utilized to simplify the account and discussion of results). The R_p then increased linearly with the Al content increasing from 20 vol.% to 40 vol.%. The change of R_p for Zn–Al films is moderate when Al is between 40 vol.% and 80 vol.%, whose R_p is expected to fall into of the range between 1.5×10^4 Ω/cm^2 and 2×10^4 Ω/cm^2. The R_p resumes increasing at a faster rate after Al is more than 80 vol.%. The peak of R_p is at about 87.5 vol.% Al, but a pure Al film shows some decline in R_p. A three-stage evolution of R_p can be concluded from the data: the low R_p stage (high Zn), the medium R_p stage (middle range) and the high R_p stage (high Al). Films corresponding to the medium or high R_p stage will exhibit a good anti-corrosion performance as predicted by Eq. (1). This can be attributed to an increased completeness and uniformity of aluminum oxide resulting from both a small rich-Al grain size and a low Zn content [20].

It is generally believed that the corrosion potential E_{corr} of a metallic coating should be at least 0.3 V negative to that of the substrate to provide an effective sacrificial protection in the corrosion environment [21]. Principally, if macro defects develop in noble films, these films cannot provide enough anode protection to the bare substrates and will lead to a severe local corrosion in the substrates. As shown in Fig. 6, the E_{corr} increases sharply from −0.97 V to −0.66V (versus SCE) when the Al content exceeds from 80 vol.% to 100 vol.%. While the E_{corr} for the mild carbon steel substrate used in this research is −0.58 V, it is required that the corrosion potential for protective film should be less than −0.88 V. Considering this important factor, the Zn–Al film with Al content less than about 90 vol.% can provide satisfactory corrosion protection for steel substrates.

Potentiodynamic polarization tests were conducted on some selected samples in the Zn–Al material library. The observed polarization curves were shown in Fig. 7. It can be seen that all four samples with varied Al content show active-passive transitions, but the sample of 12.5 vol.% Al exhibits a narrower passive region and a larger passive current density compared with the other three samples. The sample containing 87.5 vol.% Al has the least passive current density and

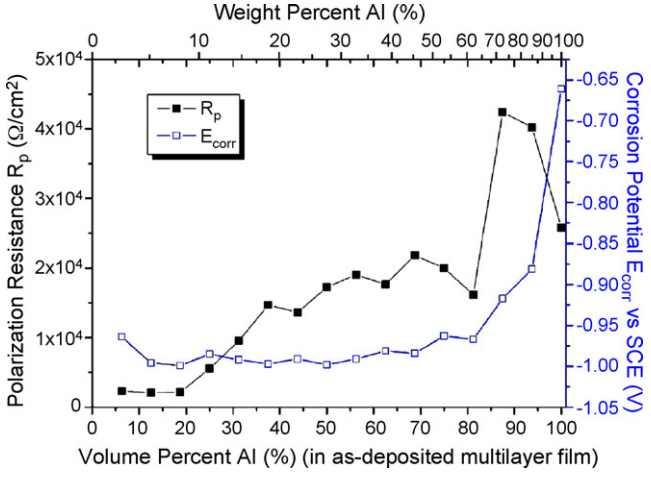

Fig. 6. Polarization resistance R_p and corrosion potential E_{corr} for samples in the Zn–Al material library as a function of Al content.

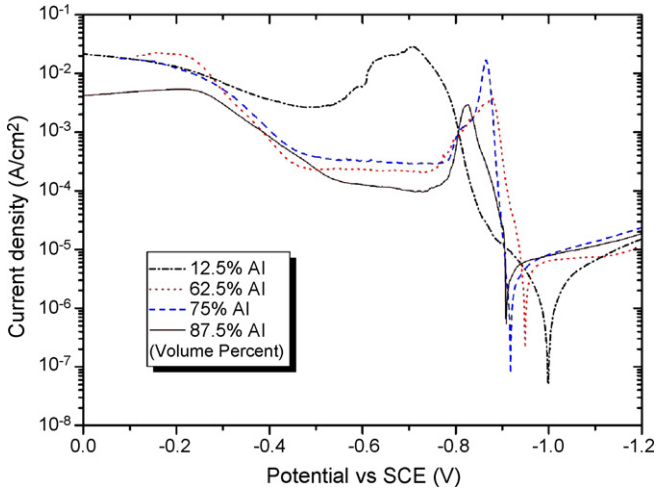

Fig. 7. Potentiodynamic polarization curves of selected samples from the Zn–Al material library.

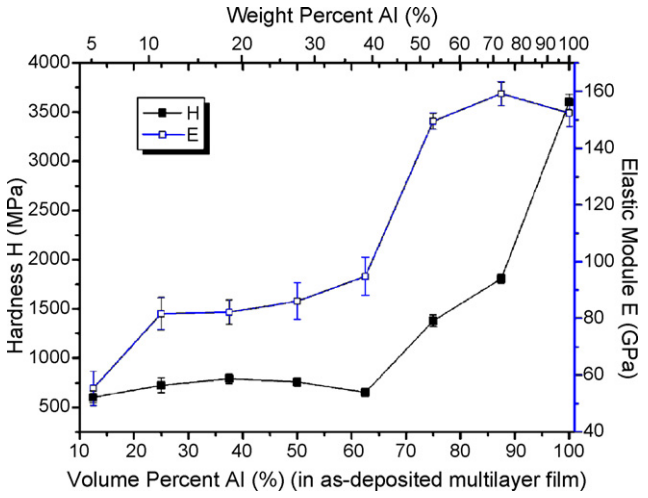

Fig. 8. Hardness H and elastic module E for samples in the Zn–Al material library as a function of Al content.

critical passive density among the three medium and high-Al samples. Combined with a relative high polarization resistance and feasible corrosion potential, it can be concluded that Zn–Al film with about 87.5 vol.% Al (equivalent to 72.8 wt% Al) has the best anti-corrosion properties in the material library.

3.3. Mechanical behaviour

Zn–Al films are applied mainly for their anti-corrosion properties, but it is also desirable that their mechanical properties can be improved to resist wear or scratch in daily usage. Fig. 8 shows the hardness and elastic module for samples in the Zn–Al material library as a function of Al content obtained by nanoindentation. The hardness of Zn–Al film does not change pronouncedly until the content of Al increased to about 50 vol.%, after which an almost linear increase of hardness was observed. The elastic module E shows a similar upward trend as the increase of Al content, but there is a plateau rather than a linear increase over the high-Al range (>70 vol.%). It is obvious that Zn–Al films containing a high Al content have better mechanical properties compared with the high Zn ones. As the Zn–Al alloy system does not form intermetallics or undergone a structure transformation over the entire composition range, the deposition and annealing parameters have more important effect on the observed mechanical properties of the material library. Ion beam sputtering can produce high quality films having excellent adhesion and high density [22], so the films exhibit improved the mechanical properties compared with conventional hot-dip or electrochemical deposition coatings. Combinatorial material library can be utilized to screen or find film compositions for better mechanical properties.

4. Conclusions

A combinatorial method was utilized to fabricate a Zn–Al material library by ion beam sputtering. The material library was fabricated by manipulating the position of substrate and moving shutters to deposit multilayer metal films with varied Al or Zn content. Different annealing conditions were studied to figure out the optimum temperature and high quality alloy films can be obtained by annealing at 370 °C. The effect of composition on the mechanical and corrosion properties of PVD Zn–Al films was studied from the material library.

Electrochemical corrosion properties were measured with by a modified tape test. Polarization resistance and corrosion potential were screened for the entire materials library. Potentiodynamic polarization tests were conducted on selected samples. There can be expected a medium or high polarization resistance and a feasible corrosion resistance for Zn–Al films containing about 35–75 wt% Al. Zn–Al film of about 72.6 wt% Al has the best overall anti-corrosion properties in the material library. Nanoindentaion tests were utilized to investigate the mechanical behaviour. Zn–Al films containing high Al content show better mechanical properties with high hardness and elastic module.

The combinatorial material library fabricated in this research can be employed to screen and optimize the alloy film composition for better corrosion and mechanical performance. The sample amount on the material library can be simply increased by reducing the sample dimension or enlarging the substrate size. It can thus improve the material research efficiency more eminently.

Acknowledgement

The authors gratefully acknowledge the Shanghai Municipal Commission of Science and Technology for financial support to this project (Grant no. 055211005).

References

[1] Z. Panossian, L. Mariaca, M. Morcillo, S. Flores, J. Rocha, J.J. Pena, F. Herrera, F. Corvo, M. Sanchez, O.T. Rincon, G. Pridybailo, J. Simancas, Surf. Coat. Technol. 190 (2005) 244–248.
[2] W. Miao, I.S. Cole, A.K. Neufeld, S. Furman, J. Electrochem. Soc. 154 (2007) C7–C15.
[3] A.R. Moreira, Z. Panossian, P.L. Camargo, M.F. Moreira, I.C. da Silva, J.E.R. de Carvalho, Corros. Sci. 48 (2006) 564–576.
[4] E. Palma, J.M. Puente, M. Morcillo, Corros. Sci. 40 (1998) 61–68.
[5] P.R. Sere, M. Zapponi, C.I. Elsner, A.R. Di Sarli, Corros. Sci. 40 (1998) 1711–1723.
[6] X. Xiao, Y.Q. Long, P. Zhong, L. Wu, Corros. Protect. 26 (2005).
[7] T. Maruyama, T. Kobayashi, M. Kano, Mater. Trans. 47 (2006) 1853–1858.
[8] A.R. Marder, Prog. Mater. Sci. 45 (2000) 191–271.
[9] L. Li, W.B. Nowak, J. Vac. Sci. Technol. A 12 (1994) 1587–1594.
[10] L. Guzman, G.K. Wolf, G.M. Davies, Surf. Coat. Technol. 174 (2003) 665–670.
[11] J. Cui, Y.S. Chu, O.O. Famodu, Y. Furuya, J. Hattrick-Simpers, R.D. James, A. Ludwig, S. Thienhaus, M. Wuttig, Z.Y. Zhang, I. Takeuchi, Nat. Mater. 5 (2006) 286–290.
[12] Y.K. Yoo, T. Ohnishi, G. Wang, F. Duewer, X.D. Xiang, Y.S. Chu, D.C. Mancini, Y.Q. Li, R.C. O'Handley, Intermetallics 9 (2001) 541–545.
[13] S.M. Han, R. Shah, R. Banerjee, G.B. Viswanathan, B.M. Clemens, W.D. Nix, Acta Mater. 53 (2005) 2059–2067.
[14] T. Hakkarainen, Proceedings of the Symposium Laboratory Corrosion Tests and Standards, Bal Harbour, FL, ASTM STP 866, 1983, pp. 91–107.
[15] W.C. Oliver, G.M. Pharr, J. Mater. Res. 7 (1992) 1564–1580.

[16] A. Rar, E.D. Specht, E.P. George, M.L. Santella, G.M. Pharr, J. Vac. Sci. Technol. A 22 (2004) 1788–1792.
[17] F.H. Wohlbier, Diffusion and Defect Data, Aedermannsdorf/Trans Tech, Bay Village, OH, Switzerland, 1974.
[18] Z.T. Liu, M. Boisson, O.N.C. Uwakweh, Metall. Mater. Trans. A: Phys. Metall. Mater. Sci. 27 (1996) 2904–2910.
[19] D.A. Jones, Principles and Prevention of Corrosion, Prentice Hall, Upper Saddle River, NJ, 1996.
[20] W.B. Nowak, L.E. Burns, V.G. Harris, J. Vac. Sci. Technol. A 7 (1989) 2350–2354.
[21] I.O. Suzuki, Corrosion-Resistant Coatings Technology, M. Dekker, New York, 1989.
[22] T. Serikawa, M. Henmi, T. Yamaguchi, H. Oginuma, K. Kondoh, Surf. Coat. Technol. 200 (2006) 4233–4239.